



Belle II status and prospect *

Yoshiyuki Onuki

(On behalf of the Belle II Collaboration)

Department of Physics, The University of Tokyo, 7-3-1 Hongo, Bunkyo-ku, Tokyo, Japan
and

Systems Engineering and Science, Shibaura Institute of Technology, 307 Fukasaku, Minuma-ku, Saitama City, Saitama, Japan

Abstract

The Belle II experiment at the SuperKEKB accelerator is the upgraded successor one of the original B -factories, the Belle experiment and KEKB accelerator. The instantaneous luminosity is designed to $6 \times 10^{35} \text{ cm}^{-2}\text{s}^{-1}$ which is 30 times higher than the KEKB. We aim to accumulate 50 ab^{-1} of the data by the early 2030s to discover new physics beyond the Standard Model. The current integrated luminosity has so far reached 213 fb^{-1} by summer 2021. Belle II can also provide various physics subjects: beauty, charm, τ -lepton, dark sector and hadron physics. We confirm the detector performance as is expected. Several physics results have already appeared. We briefly report the status and prospect of the Belle II experiment.

Keywords: Super B -factory, Flavor physics, Beauty, Charm, τ , CKM, $\sin 2\phi_1$, $\sin 2\beta$, CP violation, BSM, ALPs, Z'

1. Introduction

It was proposed that the origin of the charge-parity (CP) symmetry violation in the weak interaction is caused by an irreducible complex phase(s) in the flavor changing unitary matrix [1] in 1972. The B meson was found to be a fertile place to study the CP violation mechanism in the early 80's [2] and an idea that the boosted B meson system produced by asymmetric energy e^+e^- collider was proposed to verify this experimentally. Two B meson factories, BaBar and Belle experiments had been constructed in the 90's to verify the predicted large CP violation in the B meson system. In 2002, the CP violation in the B meson system had been discovered by both experiments and verified. Because the cross sections of $\sigma(e^+e^- \rightarrow c\bar{c}) = 1.3 \text{ nb}$ and $\sigma(e^+e^- \rightarrow \tau^+\tau^-) = 0.9 \text{ nb}$ are comparable

to the $\sigma(e^+e^- \rightarrow \Upsilon(4S)) = 1.1 \text{ nb}$, the B -factories are also charm and τ -factories. Many measurements have been made by the B -factories over 20 years. Among them, discoveries in the exotic hadrons, such as heavy quarkonium-like X , Y and Z states, are notable achievements by the B -factories [3].

2. SuperKEKB accelerator and Belle II experiment

The Belle II experiment and SuperKEKB accelerator is the successor of the Belle experiment and KEKB accelerator, which is designed to explore physics beyond the Standard Model using a 50 times larger statistics of that recorded by Belle. The SuperKEKB accelerator adopts the nano beam scheme, which can provide a 30 times instantaneous luminosity of $6 \times 10^{35} \text{ cm}^{-2}\text{s}^{-1}$ [5]. The Belle II detector [4] is a multi purpose spectrometer composed of new sub-detectors as shown in Fig. 1. The innermost detector is the vertex detector (VXD), which consists of two inner layers of silicon pixel detector (PXD) and four outer layers of double-sided silicon strip detector (SVD). The tracking detector is a 56

*Belle II status and prospect talk presented at QCD21, 24th International Conference in QCD (5-9/7/2021, Montpellier - FR).

Email address: yoshiyuki-onuki@g.ecc.u-tokyo.ac.jp
(Yoshiyuki Onuki
(On behalf of the Belle II Collaboration))

layers of drift wire chamber (CDC). Two types of ring-imaging Cherenkov detectors are used as particle identification detectors, time of propagation detector using quartz in the barrel region (TOP) and focusing aerogel RICH at the forward end-cap region (ARICH). CsI(Tl) crystals for the electromagnetic calorimeter surrounds the barrel and both the end-cap region. The superconducting magnet provides 1.5 T field and contains the detectors described above. The K_L and μ detector is composed of super-layers of iron sandwiched by resistive plate chamber or plastic scintillator detector(KLM). The front-end system of sub-detectors except for the PXD are in a common DAQ framework. The trigger logic combines information from CDC, TOP, ARICH, ECL and KLM within the 5 μ s latency at a maximum frequency of 30 kHz. Data from sub-detectors are merged in an event by the event builder PC farm. To reduce the huge amount of data from PXD, there is an extra feedback path in the PXD data acquisition to realize partial readout in a region of interest defined by tracks interpolated from the SVD and CDC to the surface of the PXD. The raw data is stored at the KEK, as well as a replica in the Brookhaven National Laboratory; data processing is performed at both sites. The data are distributed to the regional data centers and processed by GRID sites around the world.

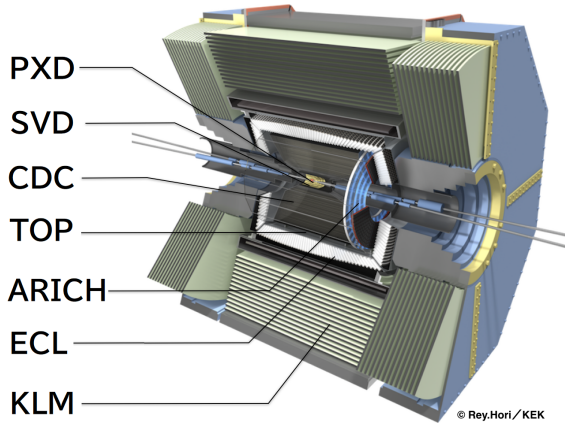


Figure 1: Schematic of the Belle II detector.

The SuperKEKB accelerator is an asymmetric energy e^+e^- collider having a capability to scan the collision energy from just below the $\Upsilon(1S)$ to just above the $\Upsilon(6S)$. For the $\Upsilon(4S)$ run, the e^+ and e^- beam energies are 4 GeV and 7 GeV, respectively. The instantaneous luminosity L is provided by the formula

$$L = \frac{\gamma_{\pm}}{2er_e} \left(1 + \frac{\sigma_y^*}{\sigma_x^*}\right) \left(\frac{I_{\pm} \xi_{y\pm}}{\beta_y^*}\right) \left(\frac{R_L}{R_{\xi_{y\pm}}}\right), \quad (1)$$

where \pm denotes positron(+)-electron(-) beam, respectively. Here $\sigma_{x(y)}^*$ is the beam size at the interaction point(IP) in the horizontal(vertical) plane. I is the beam current, β_y^* is the vertical beta function at the IP, $\xi_{y\pm}$ is the vertical beam-beam parameter, R_L and $R_{\xi_{y\pm}}$ are the reduction factors for the luminosity and the beam-beam parameter, r_e is the classical electron radius, and γ is the Lorentz factor. The nano-beam scheme strongly squeezes the β_y^* from 5.9 mm in the KEKB to 0.3 mm at the IP region. This is expected to increase luminosity by a 20 times that of KEKB. Keeping a low emittance is necessary in this scheme so a new dumping ring for the positron injection was constructed and has been operating since 2018. With a 1.5 times increase of beam current, the total increase of a 30 times is expected. The expected luminosity is shown in the Fig. 3. In 2022, we will have a long shutdown (LS1) for the full installation of the second PXD layer and exchange of TOP photomultiplier tubes. In 2026, we are planning LS2 for an interaction region upgrade so the design luminosity can be obtained. By around 2030, a data set corresponding to 50 ab^{-1} of integrated luminosity is planned. The main goal of the Belle II experiment is to discover beyond the Standard Model and indicate a new physics model. There are many promising and interesting modes, which are summarized in [6], including τ , charm, hadron physics, dark sector and etc.

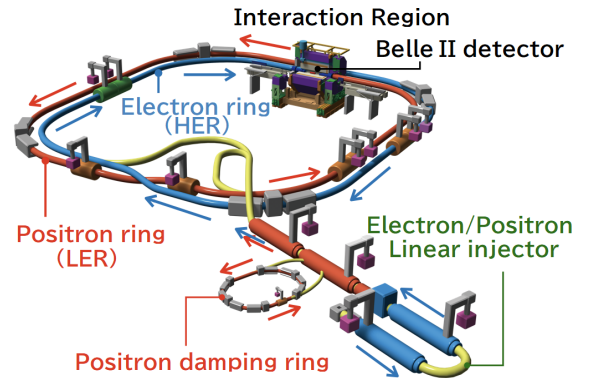


Figure 2: Schematic of the SuperKEKB accelerator.

3. Status of the Belle II experiment

SuperKEKB and Belle II project had started in 2012. In 2016, SuperKEKB had started its commissioning. Beams only stored in both rings, with neither collisions nor the Belle II detector. After this success, Belle II detector, without VXD, was rolled in to the IP region

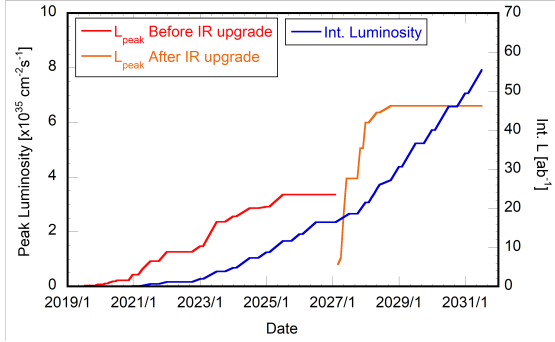


Figure 3: Luminosity projection in the next decade.

and a pilot physics run with beam collision started in 2017. During the run, 472 pb^{-1} of data was accumulated. In 2018, the VXD was installed in the Belle II detector and the physics run started. Figure 4 shows the recorded physics data up to July 2021. In total, Belle II has recorded 213 fb^{-1} of physics data. The data taking efficiency of Belle II has reached $\sim 90\%$ in the latest operation. Also, SuperKEKB set a new world record for instantaneous luminosity of $3.1 \times 10^{-34} \text{ cm}^{-2} \text{ s}^{-1}$ at end of the latest physics run (June 2021).

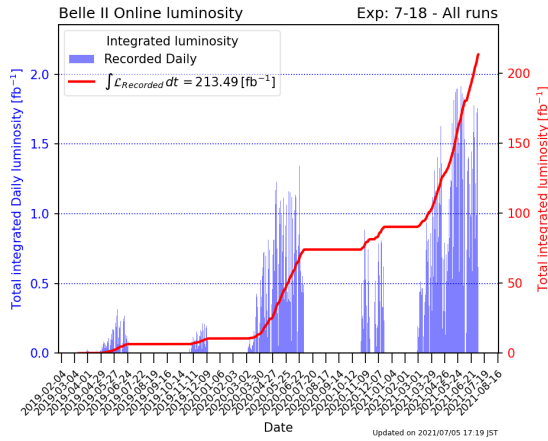


Figure 4: Recorded Belle II integrated luminosity by July 2021.

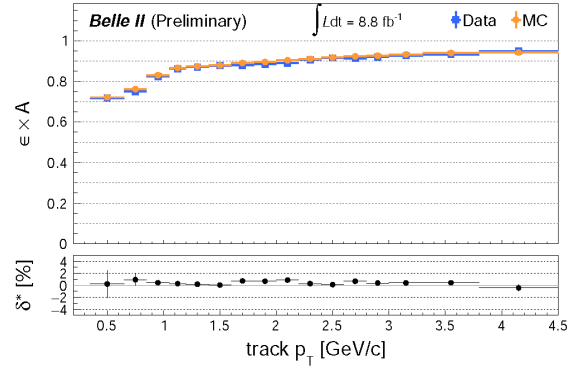
4. Detector performance

Evaluation of detector performance to deepen understanding of the detector is ongoing using both real data and Monte Carlo simulation data (MC). In this section, we pick up important topics related to the results

presented in Section 5. Other notable feature, reconstruction of neutral particles at Belle II, is presented in Ref. [7].

4.1. Track efficiency

The tracking efficiency has been measured using $e^+e^- \rightarrow \tau^+\tau^-$ followed by one τ decaying $\tau \rightarrow \ell^\pm \nu_\ell \bar{\nu}_\tau$, $\ell = e, \mu$ (1-prong) and the other decaying to $\tau \rightarrow 3\pi^\pm \nu_\tau + n\pi^0$ (3-prong). In the reconstructed 1-prong τ decay, the fraction of one charged pion missing events to the decay is equivalent to a product of tracking efficiency ϵ and the detector acceptance A . The efficiency and the calibrated discrepancy δ^* between the data and MC are evaluated in terms of the transverse momentum of the 1-prong track as shown in Fig. 5. The data and MC agree well with only a small correction required.

Figure 5: Measured product of tracking efficiency ϵ and detector acceptance A with calibrated Data-MC inconsistency δ^* .

4.2. Particle identification

Particle identification (PID), is performed for each particle using the detected information from CDC, TOP, ARICH, ECL and KLM. These likelihoods are used to construct a combined likelihood ratio. The binary charged kaon/pion likelihood ratio can be defined by $\mathcal{R}_{K/\pi} = \mathcal{L}_K / (\mathcal{L}_K + \mathcal{L}_\pi)$. The PID performance was evaluated using a sample of $D^{*+} \rightarrow D^0[K^-\pi^+]\pi^+$ decays collected from both on resonance (34.6 fb^{-1}) and off resonance (60 MeV below the $\Upsilon(4S)$, 2.4 fb^{-1}) data [8]. The kaon identification efficiency ϵ_K is defined as: $\epsilon_K = (\text{number of kaon tracks identified as kaon}) / (\text{number of kaon tracks})$ while the pion mis-identification rate is defined as: $\pi \text{ mis-ID rate} = (\text{number of pion tracks identified as kaon}) / (\text{number of pion tracks})$. Figure 6 shows the results for ϵ_K and pion mis-identification rate as function of the momentum.

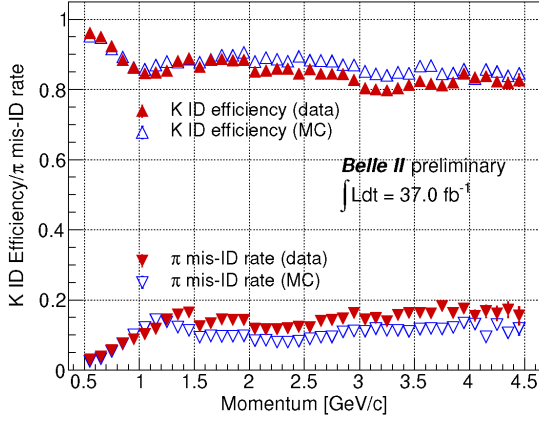


Figure 6: Kaon efficiency and pion mis-identification rate for the criterion $\mathcal{R}_{K/\pi} > 0.5$ using the decay $D^{*+} \rightarrow D^0[K^-\pi^+]\pi^+$.

4.3. Flavor tagging

In time-dependent CP violation analysis, one of the two neutral B mesons is reconstructed in the specific CP eigenstate decay of interest. Flavor tagging is a determination of the other neutral B -meson (tag-side), B^0 or \bar{B}^0 , from the final state particles without reconstructing the decay. The algorithm is a necessary tool for the analysis and high tagging efficiency is demanded. A flavor tagging algorithm using FastBDT is developed in Belle II [9]. The algorithm was trained by the flavor specific hadronic decays, $B^0 \rightarrow D^{(*)-}h^+$ ($h = \pi, \rho, a_1$) followed by $D^{*-} \rightarrow \bar{D}^0\pi^-$, $D^- \rightarrow K^+\pi^-\pi^-, K_S\pi^-, K_S\pi^-\pi^0, K^+\pi^-\pi^-\pi^0$ and $\bar{D}^0 \rightarrow K^+\pi^-, K_S\pi^+\pi^-, K^+\pi^-\pi^0, K^+\pi^-\pi^+\pi^-$ using MC and the real data corresponding to 8.7 fb^{-1} . The output of the algorithm is an index of the flavor tagging quality which is defined by a product of flavor charge q and the dilution factor $r_{FBDT} \in [0, 1]$, where $q = +1/-1$ when there is a B^0/\bar{B}^0 in the tag-side, respectively. If one obtains the $q \cdot r_{FBDT} = 1$, the B meson on the tag-side is unambiguously a B^0 . If one obtains $q \cdot r_{FBDT} = 0$, the flavor is undetermined. The r_{FBDT} can be expressed $r_{FBDT} = 1 - 2w$, where w is the wrongly assigned flavor fraction. Figure 7 shows the obtained $q \cdot r_{FBDT}$ distribution. The flavor tagging efficiency is estimated to be $(33.8 \pm 3.9 \text{ (stat)} \pm \text{(syst)})\%$ in comparison to $(30.1 \pm 0.4)\%$ in Belle [3].

5. Recent physics results

5.1. $\sin 2\phi_1$ measurement

Using 34.6 fb^{-1} of data, a first measurement of time-dependent CP violation and $B^0 - \bar{B}^0$ mixing are conducted for the CP eigenstate $B^0 \rightarrow J/\psi K_S$ decay and

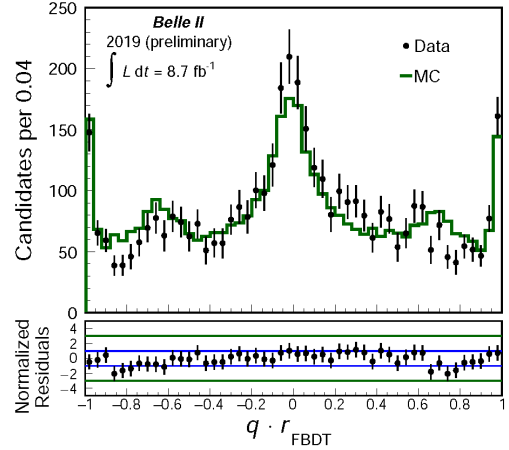


Figure 7: The $q \cdot r_{FBDT}$ distribution using $B^0 \rightarrow D^{(*)-}h^+$.

flavor specific $B^0 \rightarrow D^-\pi^+$ decay, respectively [10]. One B meson is fully reconstructed as a signal decay. For the associated B meson, the specific decay is not reconstructed but the decay vertex and the flavor information are reconstructed using the rest of tracks used for fully reconstructed B meson. The distance between the vertexes of two B mesons along the boost direction of the $\Upsilon(4S)$ can be converted to the proper-time interval Δt . The flavor of the tag-side is determined by the flavor tagger described in Sec. 4.3. Using this tagging information, we can define the asymmetry for $B^0 \rightarrow D^-\pi^+$ decays.

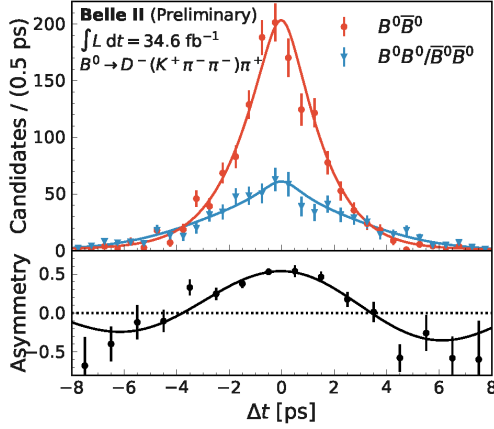
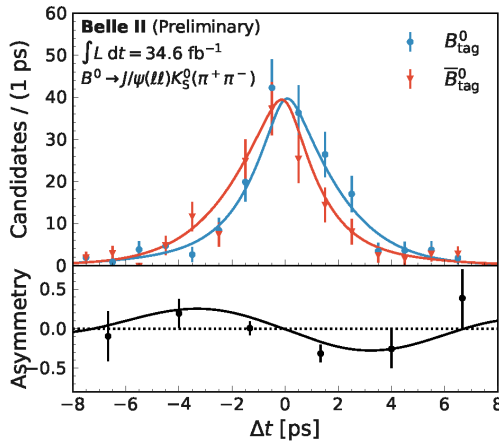
$$A_{mix}(\Delta t) \equiv \frac{N(B^0\bar{B}^0) - N(B^0B^0/\bar{B}^0\bar{B}^0)}{N(B^0\bar{B}^0) + N(B^0B^0/\bar{B}^0\bar{B}^0)} = (1 - 2w) \cos(\Delta m_d \Delta t), \quad (2)$$

where Δm_d is the mass difference of mixing and w is the wrong flavor tag fraction. Time-dependent mixing analysis is conducted using Eq. 2 and Fig. 8 shows the fit result, which gives $\Delta m_d = (0.531 \pm 0.046 \text{ (stat)} \pm 0.013 \text{ (syst)}) \text{ ps}^{-1}$.

When we choose $B^0 \rightarrow J/\psi K_S$ as the fully reconstruct decay, we can define the CP asymmetry

$$A_{CP}(\Delta t) \equiv \frac{N(\bar{B}_{tag}^0) - N(B_{tag}^0)}{N(\bar{B}_{tag}^0) + N(B_{tag}^0)} = \mathcal{S} \sin(\Delta m_d \Delta t) + \mathcal{A} \cos(\Delta m_d \Delta t) \quad (3)$$

where $\mathcal{S} = \sin 2\phi_1$ is an indirect CP violation parameter and \mathcal{A} is a direct CP violation parameter, which is assumed to be the standard model value of zero in this analysis. We perform a time-dependent CP violation fit using Eq. 3 for $B^0 \rightarrow J/\psi K_S$, with a probability density function convoluted with the proper-time resolution function obtained by the mixing study with $B^0 \rightarrow D^-\pi^+$. Figure 9 shows the fit result of the CP violation measurement and we obtained $\sin 2\phi_1 = 0.55 \pm 0.21 \text{ (stat)} \pm 0.04 \text{ (syst)}$. This result is consistent with the previous measurements.

Figure 8: Δt distribution and the mixing of $B^0 \rightarrow D^- \pi^+$.Figure 9: Δt distribution and CP asymmetry of $B^0 \rightarrow J/\psi K_S$.

5.2. Axion-like particle search

A pseudoscalar axion-like particle (ALP) decaying into $\gamma\gamma$ is searched for by Belle II using $445 \pm 3 \text{ pb}^{-1}$ of data [11]. The original axion is motivated by the strong CP problem but the ALP differs in that the coupling constant is independent of the mass. The process, $e^+e^- \rightarrow \gamma a$ followed by $a \rightarrow \gamma\gamma$, is used to look for a narrow axion peak in the squared invariant-mass $M_{\gamma\gamma}^2$ distribution and the squared recoiled-mass $M_{\text{recoil}}^2 = s - 2\sqrt{s}E_{\text{recoil}}^{c.m.}$ distribution. The signal yield fit is performed in the range $0.2 < m_a < 6.85 \text{ GeV}/c^2$ for the $M_{\gamma\gamma}^2$ and $6.85 < m_a < 9.8 \text{ GeV}/c^2$ for M_{recoil}^2 . The cross section can be calculated from the yield, which is converted to the coupling constant ALP-photon $g_{a\gamma\gamma}$. The obtained 95% confidence level (C.L.) upper limit of $g_{a\gamma\gamma}$ is shown in Fig. 10. Using the initial data set, Belle II set the most stringent constraint in the interval $0.2 < m_a < 1 \text{ GeV}/c^2$. Using increased luminosity, more than one order of magnitude improvement on $g_{a\gamma\gamma}$ sensitivity is expected [12].

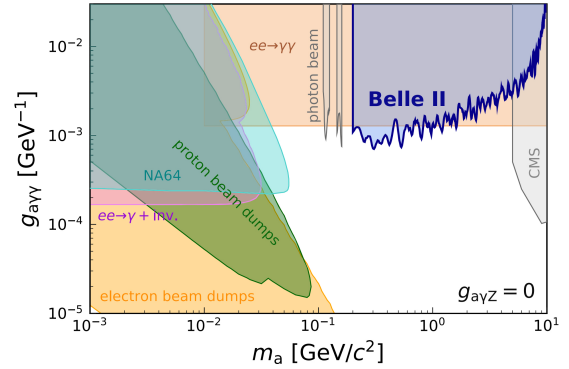


Figure 10: Obtained 95% C.L. upper limit of ALP-photon coupling.

5.3. Invisibly decaying Z' boson search

The recent $g-2$ and $b \rightarrow s\ell^+\ell^-$ anomalies motivate an additional neutral boson in the $L_\mu - L_\tau$ model [13]. The BaBar experiment searched for the $e^+e^- \rightarrow \mu^+\mu^-Z'$ followed by $Z' \rightarrow \mu^+\mu^-$ decay [14]. Belle II reported both the process $e^+e^- \rightarrow \mu^+\mu^-Z'$ and lepton flavor violating $e^+e^- \rightarrow \mu^\pm e^\mp Z'$ followed by $Z' \rightarrow \text{invisible}$ decay using 276 pb^{-1} of data [15]. The search is conducting to find a peak of Z' invariant mass in the recoil against the $\mu^+\mu^-$ or $\mu^\pm e^\mp$ pair. No excess is found. The result is translated into the coupling constant of Z' in the $L_\mu - L_\tau$ model, which leads to the 90% C.L. upper limits shown in Fig. 11.

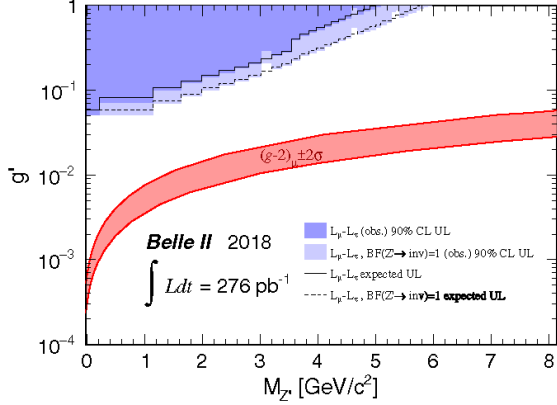


Figure 11: 90% C.L. upper limit of coupling constant g' with the favored band to explain the $g-2$ anomaly by the $L_\mu - L_\tau$ model (red).

5.4. $B^+ \rightarrow K^+ \nu \bar{\nu}$ search using inclusive tagging method

Flavor-changing-neutral-current decay is of special interests because recent measurements of $b \rightarrow s \ell^+ \ell^-$ decays having tension with the SM predictions. The $B^+ \rightarrow K^+ \nu \bar{\nu}$ decay also provides a different probe of this issue and only lepton collider experiment can make a possible measurement but it has not been observed yet. The decay is experimentally challenging because nothing except for single charged kaon from the signal B decay is reconstructed. Hence, information from the whole event, must be used for the reconstruction. The predicted branching fraction in the SM is $[4.6 \pm 0.5] \times 10^{-6}$ [16]. BaBar and Belle used semi-leptonic and hadronic approaches of reconstruction in the tag-side [17–20].

A novel inclusive tagging method is developed, which doesn't assign the explicit decay of semi-leptonic and hadronic decay in the tag-side but exploits the decay topology and kinematics with a BDT. Using the inclusive tagging method and 63 fb^{-1} of data, Belle II reported the branching fraction $[1.9^{+1.3}_{-1.3}(\text{stat})^{+0.8}_{-0.7}(\text{syst})] \times 10^{-5}$ and set the upper limit 4.1×10^{-5} at 90% C.L. in this mode [21]. The result is almost comparable to both the results of Belle [18] and BaBar [19] using the hadronic tag based on the full dataset.

5.5. D^0 and D^+ lifetime measurements

D^0 and D^+ lifetimes are measured using $e^+e^- \rightarrow c\bar{c}$ events in 72 fb^{-1} data as in Fig. 12 [22]. The D^0 and D^+ are reconstructed by $D^0 \rightarrow K^-\pi^+$ and $D^+ \rightarrow K^-\pi^+\pi^+$ candidates from $D^{*+} \rightarrow D^0[K^-\pi^+]\pi^+$ and $D^{*+} \rightarrow D^+[K^-\pi^+\pi^+]\pi^0$ decays, respectively. Due to the first layer of VXD is only 1.4 cm away from

IP in Belle II, the decay-time resolution is two times better than the Belle and BaBar experiments. These results, $\tau_{D^0} = 410.5 \pm 1.1$ (stat) ± 0.8 (syst) fs and $\tau_{D^+} = 1030.4 \pm 4.7$ (stat) ± 3.1 (syst) fs, are the most precise results and consistent with the previous measurement [23].

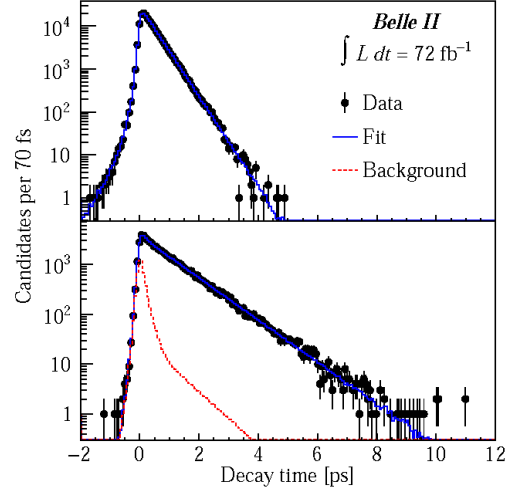


Figure 12: Decay-time distribution of $D^0 \rightarrow K^-\pi^+$ (top) and $D^+ \rightarrow K^-\pi^+\pi^+$ (bottom).

5.6. Direct CP-violation in charmless $B \rightarrow K\pi$ decays.

The difference of direct CP violation in the charmless $B \rightarrow K\pi$ decays, $\Delta\mathcal{A}_{K\pi} = \mathcal{A}_{K^+\pi^-} - \mathcal{A}_{K^0\pi^0} = 0.122 \pm 0.022$, had been observed to be nonzero, which differs from the initial expectation before the measurement was performed. This is known as the $K\pi$ puzzle and is thought to be caused by hadronic effects if there is no new physics contribution. The smoking gun test using isospin sum rule [24] was proposed by measuring the direct CP-violations and ratios of the branching fractions,

$$I_{K\pi} = \mathcal{A}_{K^+\pi^-} + \mathcal{A}_{K^0\pi^+} \frac{\mathcal{B}(K^0\pi^+)}{\mathcal{B}(K^+\pi^-)} \frac{\tau_{B^0}}{\tau_{B^+}} - 2\mathcal{A}_{K^+\pi^0} \frac{\mathcal{B}(K^+\pi^0)}{\mathcal{B}(K^+\pi^-)} \frac{\tau_{B^0}}{\tau_{B^+}} - 2\mathcal{A}_{K^0\pi^0} \frac{\mathcal{B}(K^0\pi^0)}{\mathcal{B}(K^+\pi^-)} = 0. \quad (4)$$

In particular, Belle II is expected to play an important role for the determination of the test in the modes including neutral particles K^0 and/or π^0 in the final state. The first analysis used 62.8 fb^{-1} of data for $B^+ \rightarrow K^+\pi^0$ [25] and neutral $B^0 \rightarrow K^0\pi^0$ [26]. The results are: $\mathcal{B}(K^+\pi^0) = [11.9^{+1.1}_{-1.0}(\text{stat}) \pm 1.6(\text{syst})] \times 10^{-6}$ and $\mathcal{A}_{K^+\pi^0} = -0.09 \pm 0.09$ (stat) ± 0.03 (syst) [25], $\mathcal{B}(K^0\pi^0) = [8.5^{+1.7}_{-1.6}(\text{stat}) \pm 1.2(\text{syst})] \times 10^{-6}$ and $\mathcal{A}_{K^0\pi^0} = -0.40^{+0.46}_{-0.44}(\text{stat}) \pm 0.04(\text{syst})$ [26]. These are consistent with the previous measurement. Using the

result with current world averages of the other experiments, $I_{K\pi} = -0.11 \pm 0.13$ is obtained. The precision of $I_{K\pi}$ is dominated by that of $\mathcal{A}_{K^0\pi^0}$, and Belle II will reach few % level with 50 ab^{-1} as shown in Fig. 13.

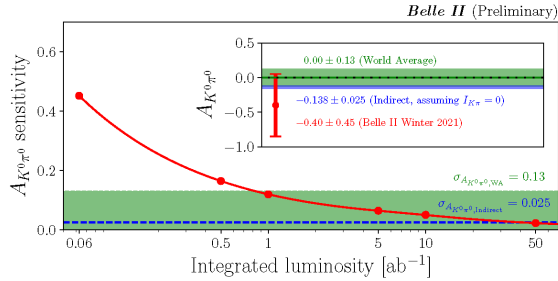


Figure 13: The projected sensitivity on $A_{K^0\pi^0}$.

6. Summary

The Belle II experiment covers a very broad range of physics using an excellent detector and large statistics. Some of the physics results show comparable or surpassing previous measurements, in spite of the smaller data taken in the early stage. We are aiming to accumulate the luminosity $\sim 400 \text{ fb}^{-1}$ comparable to BaBar experiment within this year. A lot of physics analysis is ongoing and results leading in precision will appear soon.

References

- [1] N. Cabibbo, *Unitary Symmetry and Leptonic Decays*, *Phys. Rev. Lett.* **10**, 531 (1963); M. Kobayashi and T. Maskawa, *CP Violation in the Renormalizable Theory of Weak Interaction*, *Prog. Theor. Phys.* **49**, 652 (1973).
- [2] A. B. Carter and A. I. Sanda, *CP violation in B-meson decays*, *Phys. Rev. D* **23** 1567 (1981); I. I. Bigi and A. I. Sanda, *Notes on the Observability of CP Violations in B Decays*, *Nucl. Phys. B* **193**, 85 (1981).
- [3] A. J. Bevan et al., *The Physics of the B Factories*, *Eur. Phys. J. C.* **74**, 3026 (2014).
- [4] T. Abe et al., *Belle II Technical Design Report*, arXiv:1011.0352v1.
- [5] Y. Ohnishi et al., *Accelerator design at SuperKEKB*, *Prog. Theor. Exp. Phys.* **2013**, 03A011.
- [6] E. Kou et al., *The Belle II Physics Book*, *Prog. Theor. Exp. Phys.* **2019**, 123C01.
- [7] Belle II collaboration, $\pi^0 \rightarrow \gamma\gamma$ and $\eta \rightarrow \gamma\gamma$, BELLE2-NOTE-PL-2019-019; η and η' , BELLE2-NOTE-PL-2020-003; $K_S \rightarrow \pi^+\pi^-$, BELLE2-NOTE-PL-2018-016.
- [8] Belle II Collaboration, *Kaon and Pion Identification Performance in Phase III data*, BELLE2-NOTE-PL-2020-024.
- [9] Belle II Collaboration, F. Abudinén et al., *First flavor tagging calibration using 2019 Belle II data*, BELLE2-CONF-PH-2020-004, arXiv:2008.02707v1.
- [10] The Belle II Collaboration, *Prompt measurements of time-dependent CP-violation and mixing*, BELLE2-NOTE-PL-2020-011.
- [11] F. Abudinén et al. (Belle II Collaboration), *Search for Axion-like Particles Produced in e^+e^- Collisions at Belle II*, *Phys. Rev. Lett.* **125**, 161806 (2020).
- [12] M. J. Dolan et al., *Revised constraints and Belle II sensitivity for visible and invisible axion-like particles*, *J. High Energ. Phys.* **2017**, 94 (2017).
- [13] W. Altmannshofer et al., *Explaining dark matter and B decay anomalies with an $L_\mu - L_\tau$* , *J. High Energ. Phys.* **2016**, 106 (2016).
- [14] J. P. Lees et al. (BaBar Collaboration), *Search for a muonic dark force at BaBar*, *Phys. Rev. D* **94**, 011102(R) (2016).
- [15] I. Adachi et al. (Belle II Collaboration), *Search for an Invisibly Decaying Z' Boson at Belle II in $e^+e^- \rightarrow \mu^+\mu^- (e^\pm\mu^\mp)$ Plus Missing Energy Final States*, *Phys. Rev. Lett.* **124**, 141801 (2020).
- [16] T. Blake, G. Lanfranchi, and D. M. Straub, *Rare decays as tests of the Standard Model*, *Prog. Part. Nucl. Phys.* **92** 50, (2017).
- [17] J. P. Lees et al. (BABAR Collaboration), *Search for $B \rightarrow K^{(*)}\nu\bar{\nu}$ and invisible quarkonium decays*, *Phys. Rev. D* **82** 112002, 2010.
- [18] O. Lutz et al. (Belle Collaboration), *Search for $B \rightarrow h^{(*)}\nu\bar{\nu}$ with the full Belle $\Upsilon(4S)$ data sample*, *Phys. Rev. D* **87** 111103(R), 2013.
- [19] J. P. Lees et al. (BABAR Collaboration), *Search for $B \rightarrow K^{(*)}\nu\bar{\nu}$ and invisible quarkonium decays*, *Phys. Rev. D* **87** 112005(R), 2013.
- [20] J. Grygier et al. (The Belle Collaboration), *Search for $B \rightarrow hv\bar{\nu}$ decays with semileptonic tagging at Belle*, *Phys. Rev. D* **96** 091101(R), 2017, erratum *Phys. Rev. D* **97** 099902 (2018).
- [21] F. Abudinén et al. (Belle II Collaboration), *Search for $B^+ \rightarrow K^+\nu\bar{\nu}$ decays using an inclusive tagging method at Belle II*, arXiv:2104.12624v2.
- [22] F. Abudinén et al. (Belle II Collaboration), *Precise measurement of the D^0 and D^+ lifetimes at Belle II*, submitted to *Phys. Rev. Lett.*, arXiv:2108.03216v1.

- [23] P. A. Zyla et al. (Particle Data Group), *Review of Particle Physics*, *Prog. Theor. Exp. Phys.* **2020**, 083C01.
- [24] M. Gronau, *A precise sum rule among four $B \rightarrow K\pi$ CP asymmetries.*, *Phys. Lett. B* **627** (2005) 82.
- [25] F. Abudinén et al. (Belle II Collaboration), *Measurement of branching fractions and direct CP-violating asymmetries in $B^+ \rightarrow K^+\pi^0$ and $\pi^+\pi^0$ decays using 2019 and 2020 Belle II data*, *BELLE2-CONF-PH-2021-006*, arXiv.2105.04111v1.
- [26] F. Abudinén et al. (Belle II Collaboration), *First search for direct CP-violating asymmetry in $B^0 \rightarrow K^0\pi^0$ decays at Belle II*, *BELLE2-CONF-PH-2021-001*, arXiv.2104.14871v2.